Coulomb Enhanced Superconducting Pair Correlations in the Frustrated Quarter-Filled Band.

Niladri Gomes,[1] W. Wasanthi De Silva,[2] Tirthankar Dutta,[1] R. Torsten Clay*,[2] and S. Mazumdar†,[1]

[1]*Department of Physics, University of Arizona, Tucson, AZ 85721*
[2]*Department of Physics & Astronomy and HPC² Center for Computational Sciences, Mississippi State, MS 39762*

(Dated: May 29, 2015)

A necessary condition for superconductivity (SC) driven by electron correlations is that electron-electron (e-e) interactions enhance superconducting pair-pair correlations, relative to the noninteracting limit. We report high-precision numerical calculations of the ground state within the frustrated two-dimensional (2D) Hubbard Hamiltonian for a wide range of carrier concentration ρ ($0 < \rho < 1$) per site. We find that long range superconducting pair correlations are enhanced only for $\rho \simeq 0.5$. At all other fillings e-e interactions mostly suppress pair correlations. The enhancement of pair correlations is driven by the strong tendency to local singlet bond formation and spin gap (SG) in $\rho = 0.5$, in lattices with quantum fluctuation[1–3]. We also report determinantal quantum Monte Carlo (DQMC) calculations that are in strong agreement with our ground state results. Our work provides a key ingredient to the mechanism of SC in the 2D organic charge-transfer solids (CTS), and many other unconventional superconductors with frustrated crystal lattices and $\rho \simeq 0.5$, while explaining the absence of SC in structurally related materials with substantially different ρ.

The possibility that e-e interactions can be the driving force behind SC in correlated-electron systems has been intensely investigated since the discovery of SC in the high T_c cuprates. The minimal requirements for a complete theory are, (i) the superconducting pair correlations are enhanced by e-e interactions, and (ii) pair correlations are long range. For moderate to large e-e interactions, pair correlations are perhaps best calculated numerically, which however can be done only for finite clusters. The simplest model incorporating e-e interactions is usually assumed to be the Hubbard model, which in quite general form can be written as

$$H = -\sum_{\langle ij\rangle,\sigma} t_{ij}(c^{\dagger}_{i,\sigma}c_{j,\sigma} + H.c.) + U\sum_{i} n_{i,\uparrow}n_{i,\downarrow} + \frac{1}{2}\sum_{\langle ij\rangle} V_{ij}n_i n_j. \quad (1)$$

All terms in Eq. 1 have their standard meaning. The first sum is the kinetic energy of noninteracting electrons within a 2D tight-binding model with hopping matrix elements t_{ij}; U and V_{ij} are onsite and nearest neighbor (n.n.) Coulomb interactions respectively. Existing numerical calculations within Eq. 1 on 2D lattices have failed to find enhancement of pair-pair correlations relative to the noninteracting model without making severe approximations[4].

It has sometimes been surmised that correlated-electron SC might evolve upon doping a spin-gapped semiconductor, as would occur in toy models such as a 2D lattice consisting of weakly coupled even-leg ladders[5,6]. Finding realistic 2D models with SG and enhanced pair correlations however remains challenging. In the present work we demonstrate from explicit numerical calculations on frustrated 2D lattices enhanced pair correlations evolving from a spin-gapped state at a carrier density $\rho \simeq 0.5$, far from the region most heavily investigated until now ($0.7 < \rho < 1.0$). We further point out the strong relevance of the resulting theoretical picture to real materials, in particular the 2D CTS superconductors, which were discovered earlier than the cuprates[7] but are still not understood.

There occurs an effective e-e attraction uniquely at $\rho = 0.5$, in lattices with strong quantum fluctuations, driven by charge-spin-lattice coupling. Consider the four-atom dimerized "molecule" of Fig. 1(a), with two strong intradimer bonds and one electron on each dimer. In the absence of the interdimer bond, electron populations are equal on all sites. As the interdimer electron hopping is switched on slowly, there is net migration of charge to the two center atoms, due to the attractive antiferromagnetic spin-coupling which leads to a singlet bond[3]. The charge migration is enhanced by the presence of electron-phonon (e-p) interactions[1,3]. The effective attraction is stronger than that near $\rho \sim 1$, where the tendency to such charge migration is necessarily smaller, with the neighboring sites already occupied. The charge-ordering (CO) of Fig. 1(a) in the spin-singlet state persists in the thermodynamic limit in one dimension (1D) $\rho = 0.5$, where for $V < V_c(U)$ e-e and e-p couplings act co-operatively[1] to give the spin-Peierls state

* Email address: **r.t.clay@msstate.edu**
† Email address: **sumit@physics.arizona.edu**

with the $2k_F$ bond modulations of Fig. 1(b) and (c). Phase segregation is avoided, as the key requirement for charge migration is a final state with vacancies on both sides of the singlet bond (see Fig. 1(a)). The spin-Peierls state at $\rho = 0.5$ is a *paired-electron crystal* (PEC), in which singlet-coupled n.n. singly occupied sites are separated by pairs of vacancies. Similar PECs occur in the $\rho = 0.5$ zigzag ladder (Fig. 1(d))[2] and in the 2D anisotropic triangular lattice (Fig. 1(e)) for sufficiently large lattice frustration[3]. We have not found the PEC[3] at any other ρ. The exceptional stability of the PEC at $\rho = 0.5$ is due to its commensurate structure. The PEC has been experimentally observed in a number of CTS[8,9] (see Supplemental Information).

Based on a valence bond (VB) perspective that has some overlap with Anderson's resonating valence bond[10] approach to the nearly $\rho = 1$ limit, we posit that SC is achieved in $\rho \simeq 0.5$ upon destabilization of the PEC, either due to increased frustration or very weak doping. The PEC wavefunction is dominated by covalent VB diagrams with periodic arrangement of the n.n. singlet bonds. Close to the PEC, the static CO and bond order are lost, but we anticipate the wavefunction to continue to be dominated by VB diagrams with singlet bonds between n.n. charge-rich sites, except that the arrangement of the bonds is no longer periodic. One such diagram is shown in Fig. 1(f)(i). Within Eq. 1, pairs of VB diagrams with only n.n. bonds are coupled through the diagrams with next nearest neighbor (n.n.n.) bonds, as in Figs. 1(f)(ii) and (iii). We collectively refer to diagrams with only n.n. and n.n.n. bonds as those with short bonds. There will be considerable pair tunneling in a wavefunction dominated by VB diagrams with short bonds, and we will refer to such a wavefunction as a paired electron liquid (PEL). The PEL would be most stable near $\rho = 0.5$, where the gain in kinetic energy due to pair tunneling is the largest.

We consider an anisotropic triangular lattice with $t_{ij} = \{t_x, t_y, t_{x+y}\}$. V_{ij} can similarly have three components. We express all quantities with dimensions of energy in units of t_x ($t_x = 1$). The bulk of our calculations are for $t_y \simeq 1$, with t_{x+y} only slightly smaller. This is because broken symmetries other than SC, viz., antiferromagnetism (AFM) and CO dominate at weaker frustrations[3]. We first calculate the exact wavefunctions in the lowest total spin $S = 0$ subspace for all ρ within the periodic 4×4 triangular lattice. In Fig. 1(g) we plot the total normalized contribution by the covalent VB diagrams with short bonds to the exact wavefunction as a function of ρ for several Hubbard U and V. For moderate to large e-e interactions the maximum in this contribution occurs at $\rho = 0.5$, where the wavefunction consists predominantly of VB diagrams with short bonds, indicating that VB diagrams with short bonds as in Fig. 1(f) dominate at $\rho = 0.5$.

In the PEL the occurrence of local singlets is enhanced by correlations and peaks for $\rho \simeq 0.5$. We anticipate Bose condensation of singlet pairs within the PEL state within the mechanism of SC proposed by Schafroth[11]. Without e-p coupling in Eq. 1 there is however no static SG and PEC insulating state, which suggests that a complete theory of SC will necessarily require explicit inclusions of both e-e and dynamic e-p interactions. As is however well established from studies of CDWs and SDWs, the *tendency* to the dominant instability in models containing both e-e and e-p interactions can be determined from studying correlation functions of the electronic Hamiltonian alone[12]. We have therefore performed calculations within Eq. 1 to determine if the dominance of VB diagrams with short singlet bonds at $\rho \simeq 0.5$ is accompanied by enhanced long-range superconducting pair correlations. The goal is to demonstrate that the PEL is a distinct ground-state phase and is a *precursor* to a correlated superconducting state.

We define the standard singlet pair-creation operator

$$\Delta_i^\dagger = \sum_\nu g(\nu) \frac{1}{\sqrt{2}} (c_{i,\uparrow}^\dagger c_{i+\vec{r_\nu},\downarrow}^\dagger - c_{i,\downarrow}^\dagger c_{i+\vec{r_\nu},\uparrow}^\dagger), \tag{2}$$

where $g(\nu)$ determine the pairing symmetry. We have calculated the equal-time pair-pair correlations $P_{ij} = \langle \Delta_i^\dagger \Delta_j \rangle$, for four different periodic anisotropic triangular lattices, 4×4, 6×6, 10×6 and 10×10, with the widest possible carrier densities $0 < \rho < 1$, using three different numerical techniques (see Methods). We have chosen lattices that have a closed shell configuration at ρ exactly 0.5, see also Supplementary Information. To facilitate comparison of multiple lattices and to mitigate finite-size effects, we calculate the distance dependent pair-pair correlations $P(r)$ ($r \equiv |\vec{r_i} - \vec{r_j}|$) and show here the average long-range pair-pair correlation $\bar{P} = N_P^{-1} \sum_{|\vec{r}|>2} P(r)$, where N_P is the number of terms in the sum[13].

We have found $d_{x^2-y^2}$ and d_{xy} symmetries to dominate over s-wave symmetries in our calculations. Further, for each lattice only one of the two d-wave channels is relevant; $d_{x^2-y^2}$ for 4×4 and 10×6, and d_{xy} for 6×6 and 10×10 (see Supplementary Information). The origin of this lattice dependence is currently not understood; note, however, that the distinction between $d_{x^2-y^2}$ and d_{xy} symmetries is to a large extent semantic in the strongly frustrated regime we investigate. Furthermore, it is possible that the actual pairing symmetry is a superposition of $d_{x^2-y^2}$ and d_{xy}. We have not attempted to find this superposition. Rather, for each lattice and ρ we have calculated the dominant symmetry $\bar{P}$ as a function of U. Plots of $\bar{P}$ versus U for the different lattices and ρ are given in the Supplementary Information. The complete results, summarized in Figs. 2 and 4, are remarkable: Coulomb interactions enhance superconducting pair correlations only in a narrow density range close to $\rho = 0.5$. For each lattice $\bar{P}(U)/\bar{P}(U=0) > 1$ for a single ρ that is either exactly 0.5 or one of two closest carrier fillings with closed shell Fermi level occupancy at $U = 0$. Pair

correlations are suppressed by U at all other ρ, including the region $0.7 < \rho < 1$ that has been extensively investigated in the context of cuprate SC[4]. In three of four lattices in Fig. 2 enhancement of $\bar{P}(U)$ occurs for ρ slightly away from 0.5. The magnitude of pair correlations depend on both the pair binding energy and the kinetic energy to be gained from pair delocalization; in finite lattices both quantities depend strongly on the details of the one-electron energy spectrum. We show in the Supplementary Information that for each of the four lattices the ρ at which enhanced $\bar{P}(U)$ occurs can be predicted from the known one-electron levels. Importantly, the deviation from 0.5 of the ρ at which $\bar{P}(U)$ is enhanced (excluding the 6×6 lattice where this deviation is zero) decreases monotonically with size.

Having nonzero V_{ij} affects lattice frustration minimally when all three components, V_x, V_y and V_{x+y} are nonzero. Pair-correlations for $V_x = V_y = V_{x+y}$ could be calculated only for the 4×4 lattice, where the behavior of the pair correlations is qualitatively similar to $V_{ij} = 0$, although the magnitude of the enhancement is smaller. We have found that when $V_x = V_y$, $V_{x+y} = 0$, d_{xy} pair correlations are enhanced uniquely for $\rho \simeq 0.5$. Similarly, $V_{x+y} \neq 0$, and any one of V_x, V_y nonzero enhances (suppresses) $d_{x^2-y^2}$ (d_{xy}). Overall, there is a broad parameter region over which the pair correlations remain enhanced at the same ρ where enhancement is found for $U \neq 0$. (see Supplementary Information).

The numerical ground state results are further confirmed by DQMC calculations. The sign problem is severe for large U, but up to $U = 2$ the results are reliable even for the largest β ($\beta = t_x/k_BT$) we have investigated (see Methods and Supplementary Information). Fig. 3 shows that with increasing β there occurs progressive enhancement of $\bar{P}(U)$ with increasing U, uniquely at $\rho \simeq 0.5$. As in Fig. 2, U suppresses pair correlations at all other ρ at large β. The excellent agreement between $\bar{P}(U)$ obtained from Path Integral Renormalization Group (PIRG) and DQMC indicates that while the DQMC calculations could be performed at the smallest T only for $U \leq 2$, enhanced pair correlations should be expected at even larger U. Fig. 4 summarizes the enhancement of pairing as a function of ρ for all lattices, including in the nondominant channels. As seen in Fig. 4, the dominant pairing symmetry is enhanced only for $\rho \simeq 0.5$. Pairing in the non-dominant channels is enhanced weakly for small $U \approx 1$ for some ρ, but are weakened further as U is increased.

Our computational results have direct implication for the mechanism of SC in the quasi-2D CTS. Typical superconducting CTS are the families (BEDT-TTF)$_2$X and Z[Pd(dmit)$_2$]$_2$. The number of holes (electrons) ρ per BEDT-TTF cation (Pd(dmit)$_2$ anion) is thus 0.5. The same stoichiometry is true for all superconducting (but not merely conducting) CTS with different organic molecular components. Strong e-e interaction and frustrated anisotropic triangular lattices also are common features[14,15]. Based on the crystal structures (BEDT-TTF)$_2$X are referred to as α, β, θ, κ etc. The κ-family has been investigated the most intensively, because of the proximity of magnetic phases to SC in these[14,15]. In this family, X=Cu[N(CN)$_2$]Cl (κ-Cl) is AFM at ambient pressure, X=Cu$_2$(CN)$_3$ (κ-CN) is a quantum spin liquid (QSL), and X=Cu[N(CN)$_2$]Br (κ-Br) and X=Cu(NCS)$_2$ (κ-NCS) are superconductors at ambient pressure[14]. SC is also observed in κ-Cl and κ-CN under pressure[14]. Pseudogap behavior has been observed in the "metallic" κ-Br and κ-NCS for $T < T_{PG} \sim 50$K from NMR[16–20], STM[21], precision lattice expansion[22], and magnetic torque measurements[23].

Structurally, in the κ-family the BEDT-TTF molecules are strongly coupled as dimers, which form an anisotropic triangular lattice. AFM in κ-Cl and QSL behavior in κ-CN are then easily explained if the dimers and not the individual molecules are considered as effective sites. This gives an effective $\rho = 1$ Hubbard model that will yield the AFM (QSL) for weak (strong) frustration[14,15]. Precise numerical calculations have however demonstrated the absence of SC within the $\rho = 1$ Hubbard model for any frustration[24–26]. Our present work is able to explain both the magnetic behavior and SC: in the localized insulating phase the dimerized $\rho = 0.5$ and the effective $\rho = 1$ model give same behavior[3], but in the pressure-induced delocalized phase larger interdimer hopping leads to breakdown of the effective picture and quantum critical transition from the AFM to the PEL, which is superconducting once pair coherence is reached. Strong support for this viewpoint is obtained from the recent observation of the PEC in κ-Hg(SCN)$_2$Cl[9]. Further, our proposed mechanism gives for the first time a cogent explanation of the pseudogap in κ-Br and κ-NCS. The effective $\rho = 1$ model fails to explain the $T < T_{PG}$ NMR behavior[27]. Within our theory at T_{PG} there occurs the quantum critical transition to the PEL, while phase coherence and SC are reached only at T_c. Diamagnetism observed from Nernst coefficient measurements at $T > T_c$[28] supports this picture of preformed pairs. The close proximity of the PEL to the PEC explains the density wave-like behavior in this phase noted by Müller et al.[22]. In Fig. 3, enhanced pair correlation at $\rho = 0.5$ begins to appear already at $\beta = 8$; with average $|t| \sim 0.1$ eV, we see that T_{PG} can be as high as ~ 100 K.

In other CTS, the semiconducting state proximate to SC exhibits CO. Pressure-induced SC from CO states is seen in α- and θ-(BEDT-TTF) compounds[7], EtMe$_3$P[Pd(dmit)$_2$]$_2$[8] and β-(meso-DMBEDT-TTF)$_2$X (X = PF$_6$ and AsF$_6$)[29]. The horizontal stripe CO below the SG transitions in the α- and θ-(BEDT-TTF)[30,31], the so-called valence bond crystal order in EtMe$_3$P[Pd(dmit)$_2$]$_2$[8] and the checkerboard CO in β-(meso-DMBEDT-TTF)$_2$X (X = PF$_6$ and AsF$_6$)[29] all have the same pattern as the PEC in Fig. 1(e) (see reference 32 and Supplementary Information). The bandwidth-driven quantum critical transition is now directly from the PEC to SC. The strong role of phonons in SC seen experimentally[33] is expected, as it is the co-operative effect between the e-e and e-p interactions[1,3] that drives

the transitions to the PEC and PEL.

Two of us have recently pointed out the unusual abundance[34] of seemingly unrelated correlated-electron materials that are superconducting at carrier concentration $\rho \simeq 0.5$. In all cases the superconductor belongs to a family of materials with varying ρ, and no SC is observed for ρ substantially different from 0.5 (as is also true for the CTS). While the experimental systems should be investigated individually, it is conceivable that the shared features of $\rho = 0.5$, lattice frustration and strong e-e interaction point to a new paradigm for correlated-electron SC.

Acknowledgements. This work was supported by the US Department of Energy grant DE-FG02-06ER46315 (De Silva, Dutta, and Clay) and by NSF-CHE-1151475 (Gomes and Mazumdar). Part of the calculations were performed using resources of the National Energy Research Scientific Computing Center (NERSC), which is supported by the Office of Science of the US Department of Energy under Contract No. DE-AC02-05CH11231.

Methods. Calculations used four different methods: i) *Exact diagonalization using the valence bond basis:* This exact method was used to calculate ground-state quantities for the 4×4 lattice; ii) *Path Integral Renormalization Group (PIRG):* PIRG was used to calculate ground-state pair-pair correlation functions for the 6×6 and 10×6 lattices; iii) *Constrained Path Monte Carlo (CPMC):* CPMC with a free-electron trial wavefunction was used to calculate pair-pair correlation functions for the 10×10 lattice; iv) *Determinantal Quantum Monte Carlo (DQMC):* DQMC was used to calculate pair-pair correlation functions at finite temperature for the 6×6, 10×6, and 10×10 lattices. Further details of the methods are given in the Supplementary Information.

Author Contributions. N. Gomes, W. Wasanthi De Silva, and R. T. Clay performed PIRG, CPMC, and DQMC calculations. T. Dutta performed the VB calculations. R. T. Clay and S. Mazumdar conceived of the overall project and wrote the manusctript.

Competing financial interests. The authors declare no competing financial interests.

[1] R. T. Clay, S. Mazumdar, and D. K. Campbell. The pattern of charge ordering in quasi-one dimensional organic charge-transfer solids. *Phys. Rev. B*, 67:115121, 2003.

[2] R. T. Clay and S. Mazumdar. Co-operative bond-charge density wave and giant spin gap in the quarter-filled zigzag electron ladder. *Phys. Rev. Lett.*, 94:207206, 2005.

[3] S. Dayal, R. T. Clay, H. Li, and S. Mazumdar. Paired electron crystal: Order from frustration in the quarter-filled band. *Phys. Rev. B*, 83:245106, 2011.

[4] D. J. Scalapino. A common thread: The pairing interaction for unconventional superconductors. *Rev. Mod. Phys.*, 84:1383–1417, 2012.

[5] Matthias Troyer, Hirokazu Tsunetsugu, and T. M. Rice. Properties of lightly doped t-J ladders. *Phys. Rev. B*, 53:251–267, 1996.

[6] E. Arrigoni, E. Fradkin, and S. A. Kivelson. Mechanism of high-temperature superconductivity in a striped Hubbard model. *Phys. Rev. B*, 69:214519, 2004.

[7] T. Ishiguro, K. Yamaji, and G. Saito. *Organic Superconductors.* Springer-Verlag, New York, 1998.

[8] M. Tamura, A. Nakao, and R. Kato. Frustration-induced valence-bond ordering in a new quantum triangular antiferromagnet based on $[Pd(dmit)_2]$. *J. Phys. Soc. Jpn.*, 75:093701, 2006.

[9] N. Drichko, R. Beyer, E. Rose, M. Dressel, J. A. Schlueter, S. A. S. A. Turunova, E. I. Zhilyaeva, and R. N. Lyubovskaya. Metallic state and charge-order metal-insulator transition in the quasi-two-dimensional conductor κ-(BEDT-TTF)$_2$Hg(SCN)$_2$Cl. *Phys. Rev. B*, 89:075133, 2014.

[10] P. W. Anderson. The resonating valence bond state in La_2CuO_4 and superconductivity. *Science*, 235:1196, 1987.

[11] M. R. Schafroth. Superconductivity of a charged ideal Bose gas. *Phys. Rev.*, 100:463–475, 1955.

[12] J. E. Hirsch and D. J. Scalapino. $2p_F$ and $4p_F$ instabilities in the one-dimensional Hubbard model. *Phys. Rev. B*, 29:5554–5561, 1984.

[13] Z. B. Huang, H. Q. Lin, and J. E. Gubernatis. Quantum Monte Carlo study of spin, charge, and pairing correlations in the t-t$'$-U Hubbard model. *Phys. Rev. B*, 64:205101, 2001.

[14] K. Kanoda and R. Kato. Mott physics in organic conductors with triangular lattices. *Annu. Rev. Condens. Matter Phys.*, 2:167–188, 2011.

[15] B. J. Powell and R. H. McKenzie. Quantum frustration in organic Mott insulators: from spin liquids to unconventional superconductors. *Rep. Progr. Phys.*, 74:056501, 2011.

[16] H. Mayaffre, P. Wzietek, C. Lenoir, D. D. Jérome, and P. Batail. ^{13}C NMR study of a quasi-two-dimensional organic superconductor κ-(ET)$_2$Cu[N(CN)$_2$]Br. *Eur. Phys. Lett.*, 28:205, 1994.

[17] S. M. de Soto, C. P. Slichter, A. M. Kini, H. H. Wang, U. Geiser, and J. M. Williams. ^{13}C NMR studies of the normal and superconducting states of the organic superconductor κ-(BEDT-TTF)$_2$Cu[N(CN)$_2$]Br. *Phys. Rev. B*, 52:10364, 1995.

[18] A. Kawamoto, K. Miyagawa, Y. Nakazawa, and K. Kanoda. ^{13}C NMR study of layered organic superconductors based on BEDT-TTF molecules. *Phys. Rev. Lett.*, 74:3455, 1995.

[19] M. Itaya, Y. Eto, A. Kawamoto, and H. Taniguchi. Antiferromagnetic fluctuations in the organic superconductor κ-(BEDT-TTF)$_2$Cu(NCS)$_2$ under pressure. *Phys. Rev. Lett.*, 102:227003, 2009.

[20] T. Kobayashi, Y. Ihara, Y. Saito, and A. Kawamoto. Microscopic observation of superconducting fluctuations in κ-(BEDT-TTF)$_2$Cu[N(CN)$_2$]Br by ^{13}C NMR spectroscopy. *Phys. Rev. B*, 89:165141, 2014.

[21] T. Arai, K. Ichimura, K. Nomura, S. Takasaki, J. Yamada, S. Nakatsuji, and H. Anzai. Superconducting and normal-state gaps in κ-(BEDT-TTF)$_2$Cu(NCS)$_2$ studied by STM spectroscopy. *Solid St. Comm.*, 116:679–682, 2000.

[22] J. Müller, M. Lang, F. Steglich, J. A. Schlueter, A. M. Kini, and T. Sasaki. Evidence for structural and electronic instabilities at intermediate temperatures in κ-(BEDT-TTF)$_2$X for X = Cu[N(CN)$_2$]Cl, Cu[N(CN)$_2$]Br and Cu(NCS)$_2$: Implications for the phase diagram of these quasi-two-dimensional organic superconductors. *Phys. Rev. B*, 65:144521, 2002.

[23] S. Tsuchiya, J. Yamada, S. Tanda, K. Ichimura, T. Terashima, N. Kurita, K. Kodama, and S. Uji. Fluctuating superconductivity in the strongly correlated two-dimensional organic superconductor κ-(BEDT-TTF)$_2$Cu(NCS)$_2$ in an in-plane magnetic field. *Phys. Rev. B*, 85:220506(R), 2012.

[24] R. T. Clay, H. Li, and S. Mazumdar. Absence of superconductivity in the half-filled band Hubbard model on the anisotropic triangular lattice. *Phys. Rev. Lett.*, 101:166403, 2008.

[25] L. F. Tocchio, A. Parola, C. Gros, and F. Becca. Spin-liquid and magnetic phases in the anisotropic triangular lattice: The case of κ-(ET)$_2$X. *Phys. Rev. B*, 80:064419, 2009.

[26] S. Dayal, R. T. Clay, and S. Mazumdar. Absence of long-range superconducting correlations in the frustrated $\frac{1}{2}$-filled band Hubbard model. *Phys. Rev. B*, 85:165141, 2012.

[27] E. Yusuf, B. J. Powell, and R. H. McKenzie. Antiferromagnetic spin fluctuations in the metallic phase of quasi-two-dimensional organic superconductors. *Phys. Rev. B*, 75:214515, 2007.

[28] M.-S. Nam, A. Ardavan, S. J. Blundell, and J. A. Schlueter. Fluctuating superconductivity in organic molecular metals close to the Mott transition. *Nature*, 449:584–587, 2007.

[29] T. Shikama et al. Magnetism and pressure-induced superconductivity of checkerboard-type charge-ordered molecular conductor β-(meso-DMBEDT-TTF)$_2$X (X = PF_6 and AsF_6). *Crystals*, 2:1502–1513, 2012.

[30] H. Mori, S. Tanaka, and T. Mori. Systematic study of the electronic state in θ—type BEDT-TTF organic conductors by changing the electronic correlation. *Phys. Rev. B*, 57:12023–12029, 1998.

[31] T. Ivek, B. Korin-Hamzic, O. Milat, S. Tomic, C. Clauss, N. Drichko, D. Schweitzer, and M. Dressel. Collective excitations in the charge-ordered phase of α-(BEDT-TTF)$_2$I$_3$. *Phys. Rev. Lett.*, 104:206406, 2010.

[32] R. T. Clay, S. Mazumdar, and D. K. Campbell. Charge ordering in θ-(BEDT-TTF)$_2$X materials. *J. Phys. Soc. Jpn.*, 71:1816–1819, 2002.

[33] A. Girlando, M. Masino, A. Brilliante, R. G. DellaValle, and E. Venuti. BEDT-TTF organic superconductors: The role of phonons. *Phys. Rev. B*, 66:100507, 2002.

[34] S. Mazumdar and R. T. Clay. The chemical physics of unconventional superconductivity. *Int. J. Quant. Chem.*, 2014:1053, 2014.

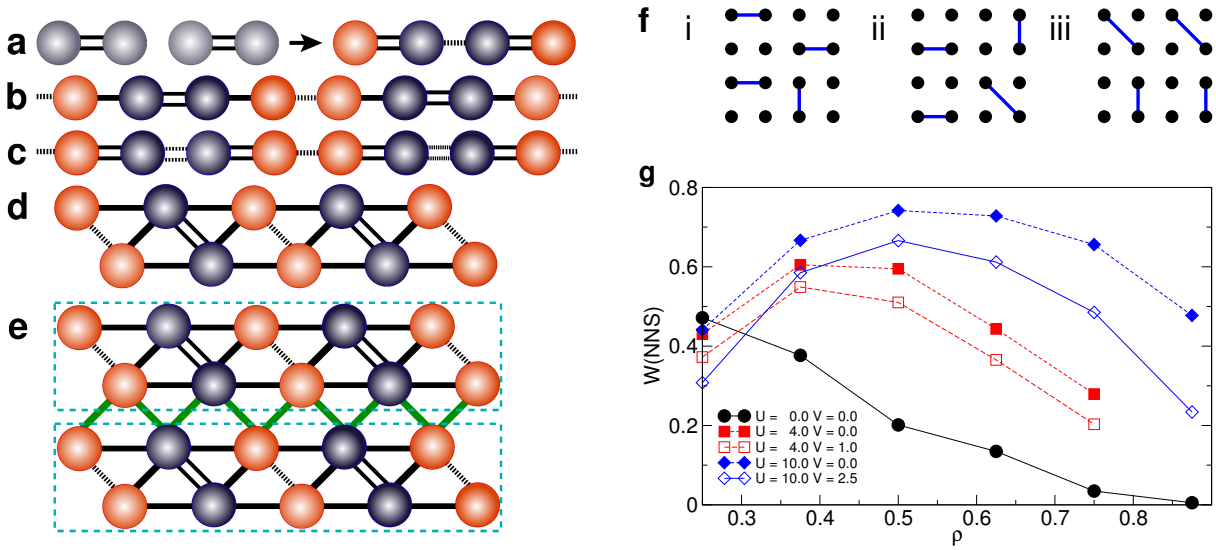

FIG. 1: **Effective e-e attraction in $\rho = 0.5$.** (a) $\rho = 0.5$ dimers with weak (left) and moderate (right) interdimer singlet bonding. Sites colored gray, blue and red have charges 0.5, > 0.5 and < 0.5, respectively. (b) and (c) $2k_F$ spin singlet states in the $\rho = 0.5$ 1D chain, for small to intermediate U and V ($U \simeq 4$, $V \simeq 1$), and for intermediate to large U and V ($U \leq 10$, $V \leq 3$) respectively. In both cases $V < V_c(U)$[1]. (d) The PEC in the $\rho = 0.5$ zigzag ladder[2]. (e) The PEC in the anisotropic 2D triangular lattice[3]. The CO has pattern ...1100... in two directions and ....1010... in the third direction, where '1' and '0' denote charge-rich and charge-poor sites. The 2D PEC has the same charge structure as would be obtained from coupled zigzag ladders. Double, single and dotted bonds in (b) – (e) denote bonds with decreasing strengths, with the double dotted bond weaker than a single bond but stronger than a single dotted bond. Differences in bond strengths result from nonzero e-p coupling. (f) Covalent VB diagrams with short bonds in $\rho = 0.5$. (g) Exact total normalized weights of covalent VB diagrams with short bonds in the ground state wavefunction of different ρ for the 4×4 lattice, for $t_y = 1$, $t_{x+y} = 0.8$.

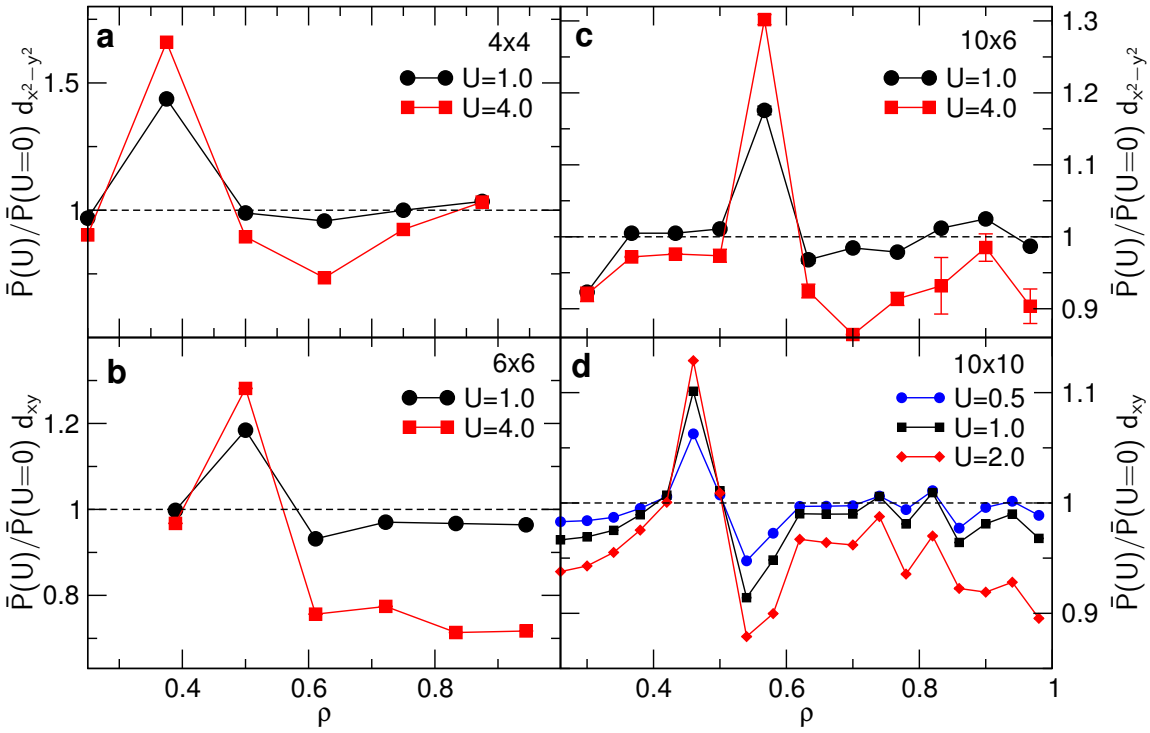

FIG. 2: **Density dependence of dominant ground state pair-pair correlations.** Average long range pair-pair correlation $\bar{P}(U)$ normalized by its uncorrelated value $\bar{P}(U=0)$, for the (a) 4×4, (b) 6×6, (c) 10×6 and (d) 10×10 anisotropic triangular lattices, for $t_y = 0.9$ and $t_{x+y} = 0.8$. The 4×4 results are exact; 6×6 and 10×6 results are obtained using the PIRG method; and 10×10 by the CPMC method. $\bar{P}(U)/\bar{P}(U=0) > 1$ for a single ρ in each case, either for $\rho = 0.5$ or for one of two closest carrier fillings with closed shell Fermi level occupancies at $U = 0$.

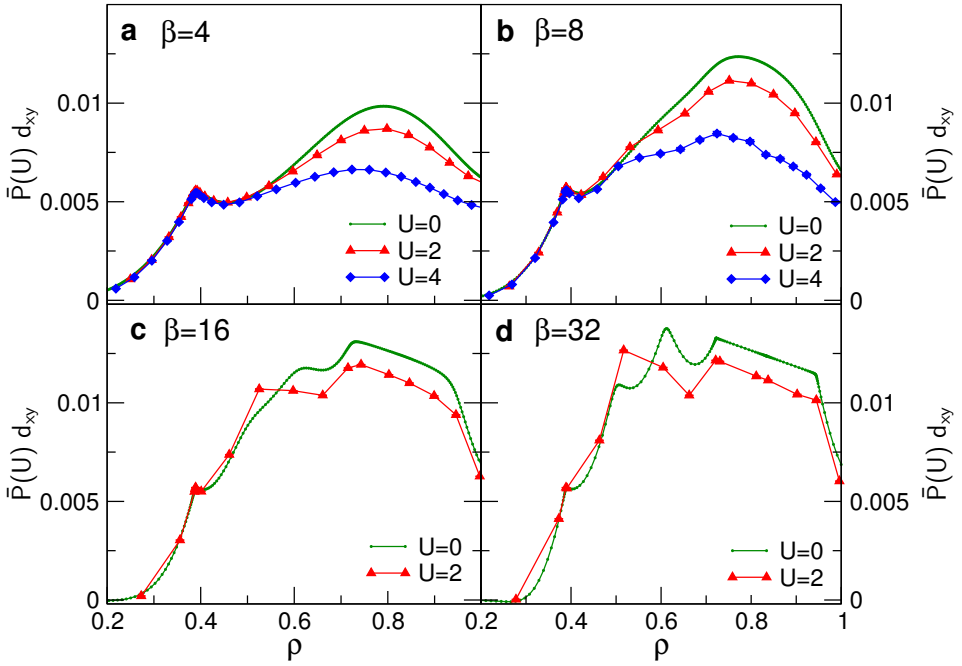

FIG. 3: **Temperature dependence of pair-pair correlations, as calculated using DQMC.** $\bar{P}(U)$ for d_{xy} pairing as a function of ρ and inverse temperature β for the 6×6 lattice with t_x =1, t_y =0.9, and t_{x+y}=0.8, calculated using DQMC. Note the gradual enhancement of $\bar{P}(U)$ for $\rho \simeq 0.5$ with increasing β, beginning from $\beta = 8$. $\bar{P}(U)$ is suppressed by U at all other ρ.

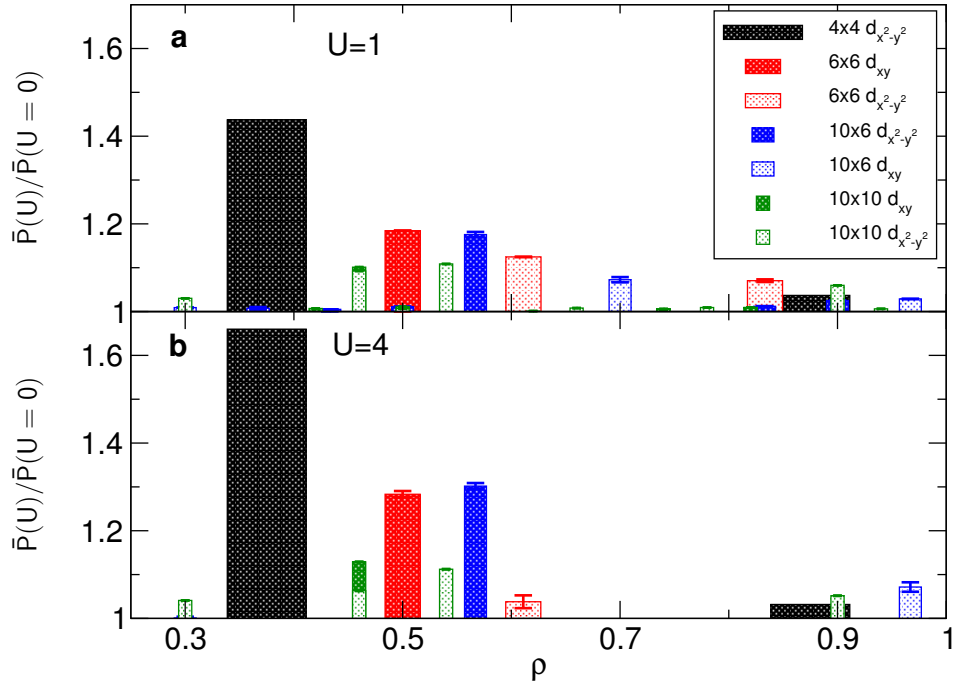

FIG. 4: **Summary of ρ-dependence of ground state pair-pair correlation enhancement.** Average long range pair-pair correlation $\bar{P}(U)$ normalized by its uncorrelated value $\bar{P}(U=0)$, for (a) $U=1$ and (b) $U=4$ ($U=2$ for the 10×10 lattice). All results with $\bar{P}(U)/\bar{P}(U=0)>1$ are included, for both $d_{x^2-y^2}$ and d_{xy} pairing symmetries. The dominant pairing symmetry for each lattice is indicated with darker shading. The width of each bar is $1/N$, where N is the number of lattice sites.